Experimental Study on a Weakly-Ionized Rarefied Arc-Jet Flowing Supersonically along a Mirror and Cusp Magnetic Field

K. Tajima[1], A. Nezu[2], H. Matsuura[2], and H. Akatsuka[1, 2]

[1]Department of Energy Sciences, Tokyo Institute of Technology, Japan

[2] Research Laboratory for Nuclear Reactors, Tokyo Institute of Technology, Japan

Abstract—We experimentally study the characteristics of supersonically flowing helium plasma along a mirror and cusp magnetic field, including the flow direction along open field lines. The plasma is initially generated by arc discharge under atmospheric pressure, followed by a supersonic expansion into a weak uniform longitudinal magnetic channel in a rarefied gas wind tunnel as a plasma expansion chamber, and finally, expanded along the mirror or cusp magnetic field. Along the mirror type magnetic field, the plasma forms a high potential region around the plasma boundary and a low potential region around the axis of the plasma. For the cusp type, we observed a dark region, which is considered to be a shock wave.

Keywords—Acceleration, arc-jet flow, mirror magnetic fields, cusp magnetic field, plasma measurements

I. INTRODUCTION

Arc-jet plasmas expanding along open field magnetic lines have been used in fundamental research as well as industrial applications. For material processing, they are used for spray coatings and an ion implantation [1, 2]. Open field lines are expected to work as a magnetic nozzle to accelerate supersonic fluid [3, 4]. Being different from mechanical nozzles, they are free from damages caused by high-temperature working fluid. Another application worth mentioning is plasma acceleration for astronautic applications to improve efficiency and specific impulse of electric propulsion for artificial satellites [5, 6]. Plasma acceleration along open field lines has been studied in various types of plasma sources, such as an arc-jet, an electron cyclotron resonance (ECR) plasma, and a helicon wave plasma, where they are suggested to be also accelerated by a potential drop in open field lines [7]. On the other hand, plasma acceleration with applied magnetic field has not been completely understood yet. Hence, it is important to investigate the mechanism of plasma acceleration along open field lines.

Simultaneously, on nuclear fusion, the formation of electric field along open field lines is much as well important. The electric potential induced along the open magnetic field has been a crucial topic, with the aim to improve the confinement characteristics of mirror devices as well as divertor regions of helical or tokamak reactors [8]. Nowadays, the feasibility of a long-legged divertor is also frequently discussed, especially lowering the thermal load to the divertor walls. For this purpose, many kinds of magnetic configuration should be considered in the long-legged divertor [9, 10]. Consequently, the effect of a mirror-type or cusp-type magnetic field should be also considered on the characteristics of plasma parameters. Therefore, it is crucial to examine variation in the electric potential along the plasma flow with respect to various magnetic-field geometries.

From the viewpoint mentioned above, we have been experimentally studying the flowing characteristics of supersonically flowing rarefied arc-jet expanding into a lower pressure vessel with diverging magnetic field [11]. We have already reported a couple of results of our study for a simple diverging magnetic field [12-14].

In this study, based on our previous study of characteristics of rarefied plasmas flowing supersonically along the simple diverging magnetic field, we report a couple of findings of characteristics of arc-jet plasmas flowing along a few kinds of configuration of magnetic field, i.e., a mirror type and cusp type magnetic field. We report the flowing characteristics of the plasma along mirror and cusp magnetic field, including its effect on the plasma space potential.

II. EXPERIMENT

A. Plasma Generator

Fig. 1 shows a schematic diagram of the rarefied gas wind tunnel as a plasma expansion chamber. Its inner diameter is 1.2 m and the length is 2 m. It is evacuated by two 20-inch oil diffusion ejector pumps, followed by a mechanical booster pump and a 12-inch oil rotary pump, whose ultimate pressure is about 1×10^{-4} Torr with its pumping speed about 16 m^3/sec. The gas wind tunnel accommodates electrodes for arc discharge and six electromagnets to confine the plasma. The magnets are also applied to stabilize the position of an anode spot of the arc discharge.

Fig. 2 shows a schematic close-up view of the plasma generator and electromagnets. The cathode is made of thoriated tungsten with 3 mm in diameter, and the anode is made of copper with 1.4 mm nozzle. Discharge conditions are as follows: DC arc current

Corresponding author: Hiroshi Akatsuka
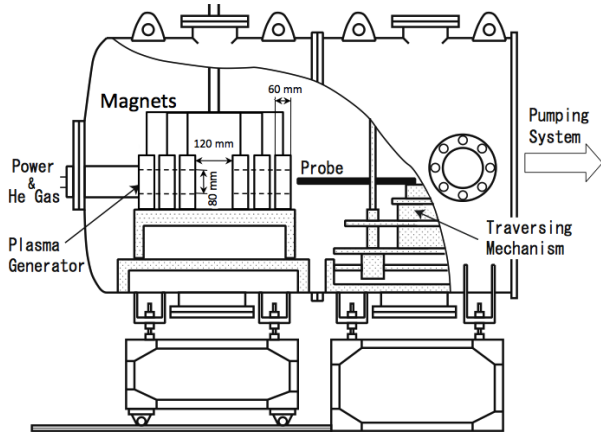e-mail address: hakatsuk@nr.titech.ac.jp

Fig. 1. Cross-sectional view of a rarefied gas wind tunnel as a plasma expansion chamber [11, 14-17].
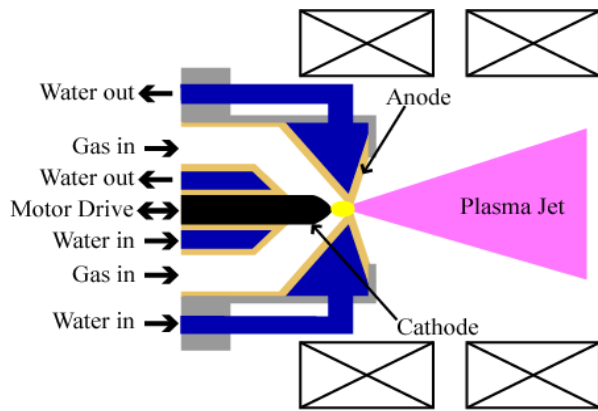

Fig. 2. Schematic diagram of an electrode assembly and plasma jet [11].

120 A, arc voltage about 16 V, and the feeding gas is helium, whose flow rate is about 0.28 L/min. Six hollow magnets are placed co-axially to the electrodes. Their inner diameter is 80 mm, and their thickness is 60 mm [15]. In the present study, we set two pairs of three magnets with their gap 120 mm, where the mirror or cusp magnetic field is generated. The plasma comes out of the anode-nozzle very stably and continuously into the hollow magnets with the help of the magnetic field. The maximum strength of the magnetic field is 0.16 T with the DC magnet current 300 A. Of course, we can choose the mirror or cusp field by the direction of the magnet current. The vector diagrams of the mirror and the cusp magnetic fields are shown in Fig. 3, where the magnet current was set at 300 A. In Fig. 3, the origin of the coordinate z is taken at the exit surface of the first three magnets. These fields were measured with a hall probe without plasma generation. Our previous research already showed that the magnetic Reynolds number Re_m of the present plasma was estimated at $Re_m \sim 0.06 \ll 1$ [14]. Therefore, the magnetic fields illustrated in Fig. 3 are almost the same as those with the arc-jet plasma flowing.
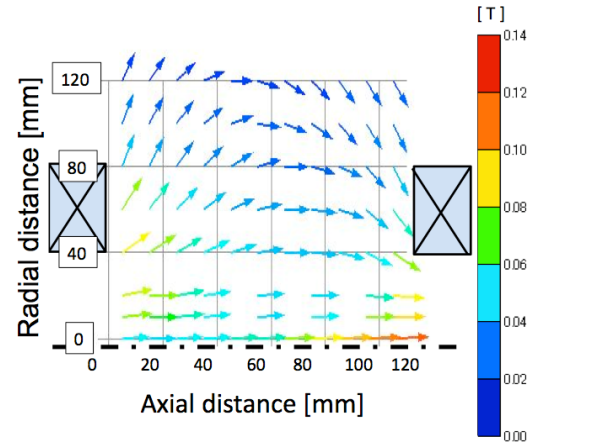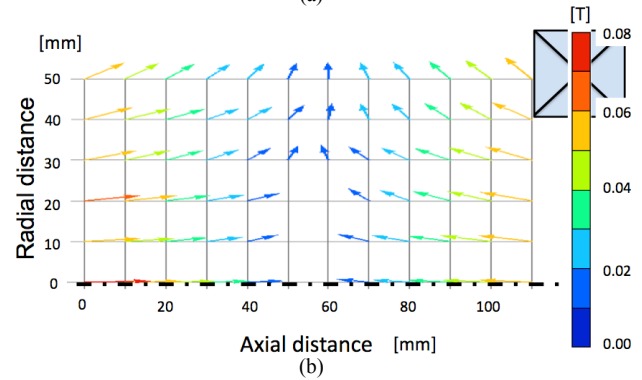
Fig. 3. Vector diagrams of (a) mirror and (b) cusp magnetic field measured by a hall probe.

B. Measurement by Mach Probe

We measured ion acoustic Mach number M_i of the plasma jet in the region of the mirror or cusp magnetic field region by a para-perp type Mach probe for supersonic flow, which has two plane electrodes facing parallel (upward to the flow) and perpendicular directions to the flow [11]. The principle of the Mach probe of the present study is described elsewhere [12]. In short, the ion Mach number M_i is calculated from the ratio of the ion saturation current of the parallel electrode to that of the perpendicular one [13]. We also applied a four-tip Mach probe to measure a two-dimensional plasma flow structure. The principle of the four-tip Mach probe is basically the same as that of the Mach probe. The electrodes are made of tungsten of 1.0 mm in diameter. The Mach probe can also be used as a general Langmuir single probe [14-16]. We can measure the electron temperature, density and plasma potential by the probe.

III. RESULTS AND DISCUSSION

A. Mirror Magnetic Field

When an arc-jet flows along the mirror magnetic field, we could observe that the plasma became bulging just along the mirror field, as in Fig. 4. On the other hand, Fig. 5 shows the vector diagrams of the ion flow and of

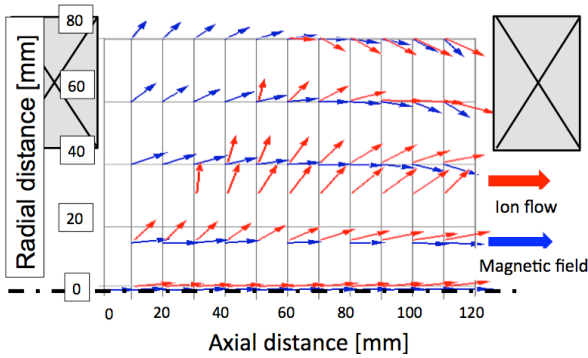Fig. 4. A photograph of the plasma flow in the mirror magnetic field.

Fig. 5. The vector diagrams of the ion flow and that of the mirror magnetic lines of force.

Fig. 6. Contour drawing of the plasma space potential in the mirror magnetic field.

the magnetic field line of force. In our previous study on the plasma flow along a simple open magnetic field, it was found that the plasma flowed almost along the magnetic field. Still, in the present mirror magnetic field, the direction of the plasma flow is considerably different, except for the plasma axis $r = 0$. However, as the plasma flows to the downstream direction, its flow direction is found to gradually come close to that of the magnetic field.

To understand this behavior, here we discuss the value of hall parameters of an electron and of an ion, which show the degree of magnetization. For example, they are $h_i = 7.06 \times 10^{-2}$ and $h_e = 5.18 \times 10^2$ for ions and of electrons, respectively, at $(r, z) = (60, 60)$ [mm]. In all other places for the present measurement, h_e is found to be always about 10^4 times larger than h_i, which indicates that the electrons are well magnetized and fully guided by the magnetic line of forces, whereas the ions are not.

The collision frequency between an electron and an ion is calculated to be $\nu_{ei} = 1.52 \times 10^6$ Hz at $(r, z) = (60, 60)$ [mm], which amounts to as about 10^5 times frequent as those between an ion and a neutral and between an electron and a neutral. These frequencies indicate that the Coulomb collisions are dominant to those with neutrals, and this tendency was confirmed all over the measurement area. Consequently, it is concluded that the electrons are fully magnetized and flow along the magnetic line of force, and they attract ions by Coulomb
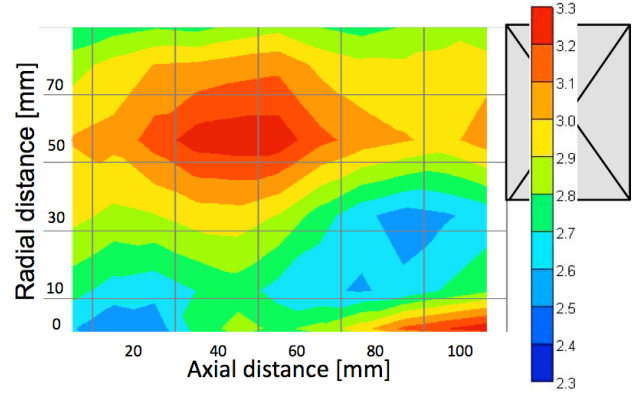
force. On the other hand, ions predominantly tend to diffuse regardless of the applied magnetic field in the upstream domain in the plasma flow field. The ions flow downstream, however, they cannot be free from the electric field that is generated by the electrons fully magnetized [11, 14-16]. And finally, the ions tend to flow with the electrons in the most downstream domain. In short, the ions-flow requires some "flowing-lag" with respect to the electron-flow.

Fig. 6 shows the space potential contour in the mirror magnetic field. On the plasma axis, it was found that the electric potential drops by 1 V as the plasma flows 100 mm to the downstream direction. Concerning the radial direction, the potential was found to lower around $r = 10$-30 mm, where higher-potential region exists. This is because the Larmor radius of ions becomes larger in the domain $z = 60$ mm with the weak magnetic field. Consequently, the hall parameter becomes even smaller, and the diffusion of ions becomes dominant and they tend to move out of the region. Meanwhile, the electrons are still well magnetized in this area, and they follow the magnetic lines of force, and do not diffuse as much as ions do. Hence, the region near $r = 30$ mm has lower space potential.

B. Cusp Magnetic Field

First, it should be remarked again that the arc-jet in the present study under atmospheric pressure before passing the anode nozzle, as shown in Fig. 2, was followed by expansion into the vacuum vessel. It is considered that the viscosity of the arc plasma before expansion chokes the anode nozzle, where the mach number of the arc-jet becomes 1 [11, 14-17]. After that, the plasma flows along a substantially uniform magnetic field, and finally, in this section, reaches the region with cusp magnetic field.

Concerning the appearance of the plasma at the cusp field, the plasma rapidly expands along the magnetic line of force. Fig. 7 shows a photograph of the plasma flow along the cusp magnetic field. We can also find a cone-shaped dark zone at about $z = 30$ mm, which is considered to be a shock phenomenon at subsonic transition, which will be discussed later.
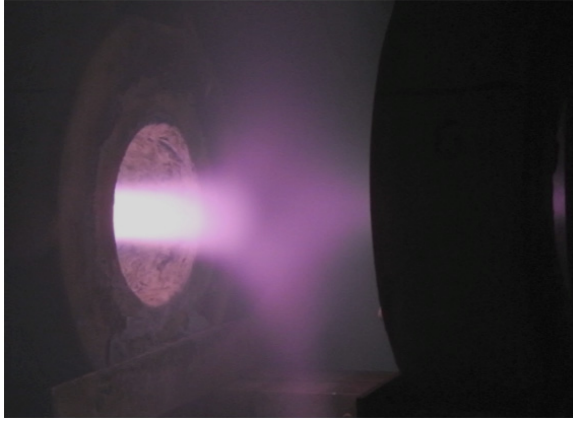
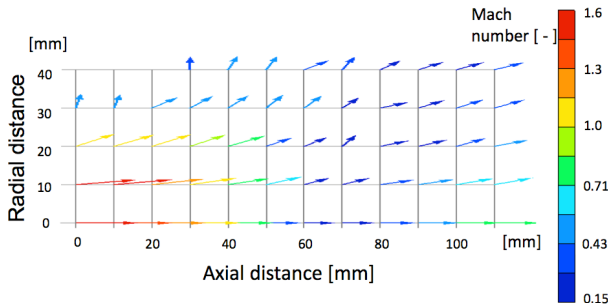Fig. 7. A photograph of the plasma flow in the cusp magnetic field.

Fig. 8. Vector diagram of the ion Mach number of the plasma flowing in the cusp magnetic field.
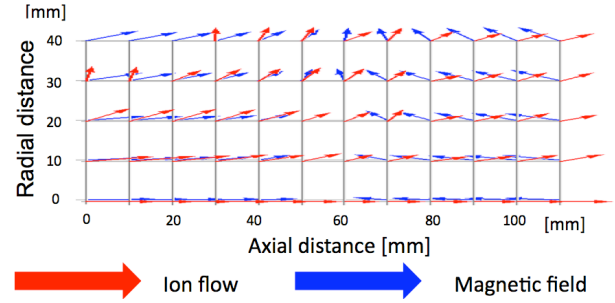

Fig. 9. Superposed vector diagrams of the ion flow (red) and that of the cusp magnetic lines of force (blue).

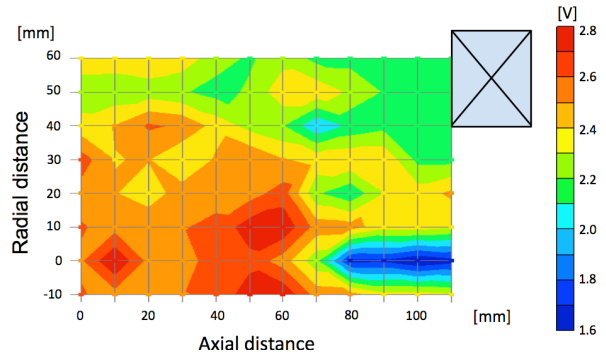Fig. 10. Contour map of the plasma space potential in the cusp magnetic field.

Fig. 8 shows a vector diagram of the ion flow in the cusp magnetic field. The value of ion Mach number is $M_i = 1.5$ at $z = 20$ mm, which indicates that the plasma is accelerated into supersonic velocity at $0 \leq z$ [mm] ≤ 20. These acceleration and deceleration phenomena can be explained qualitatively by general fluid dynamics. Fig. 8 shows that ion flow has its radial component in $0 \leq z$ [mm] ≤ 20. In other words, the cross sectional area of the plasma-flow channel increases in this region. Supersonic fluids are accelerated at diverging flowing channel with its cross sectional area A to $A + dA$, where the variation in its Mach number $M \, (\geq 1)$ is given by the following equation:

$$\frac{\mathrm{d}M}{M} = \frac{2+(\gamma-1)M^2}{2(M^2-1)}\frac{\mathrm{d}A}{A}, \qquad (1)$$

where γ is the heat capacity ratio [18]. Equation (1) can qualitatively explain the acceleration of the present plasma flow at $0 \leq z$ [mm] ≤ 20 [11, 14, 15]. However, quantitative application of (1) is still difficult in the present experiment, since the ions are not magnetized and the cross sectional area of the ion flow cannot be calculated from the variation in the strength of the magnetic field.

The dark zone observed at $z = 30$ mm is considered to be the shock front, not only because this position corresponds to the subsonic transition, but also because the electron temperature and density change drastically at this surface.

Fig. 9 is a diagram of superposed vector of the ion Mach number and the magnetic lines of force. It is found

that the direction of both vectors agrees well for the region $0 \leq z$ [mm] ≤ 60 and r [mm] ≤ 20, while the ions tend to diffuse wider than the magnetic field for $r \geq 20$ mm. It should be also noted that the discrepancy of both vectors becomes more evident at $z \geq 60$ mm due to the cusp field. And after passing the separatrix, the direction of an ion flow becomes anti-parallel to the magnetic field, and finally, again the ion flows along the magnetic lines of force.

Based on discussion on the plasma parameters in the cusp field, let us examine the variation in the hall parameters in this field. As an example of the upstream domain, at $(z, r) = (20, 30)$ [mm], the hall parameters of ions and electrons are $h_i = 1.63 \times 10^{-2}$ and $h_e = 1.19 \times 10^2$, respectively. On the other hand, at $(z, r) = (90, 30)$ [mm] in the downstream domain, $h_i = 8.71 \times 10^{-3}$ and $h_e = 6.4 \times 10$, respectively, which indicates that in both regions, electrons are well magnetized but ions are not. At the same time, just near the saddle point of the magnetic field $(z, r) = (50, 30)$ [mm], $h_e = 2.7$, which means that the even magnetization of electrons becomes also weak in the central region in Figs. 8 and 9.

Fig. 10 shows a contour of the plasma space potential. It is found that the electric potential reaches its maximum near the saddle point of the field. In addition, we found that the space potential drops by about ~ 1 V as the plasma flows to the downstream direction along the axis, from $z = 50$ mm to 100 mm. First, let us confirm the reason for the high space potential near the saddle point. Fig. 11 shows another contour map for the value of the ion velocity. In Fig. 11, we consider only the absolute value of the velocity and do not discuss the direction.
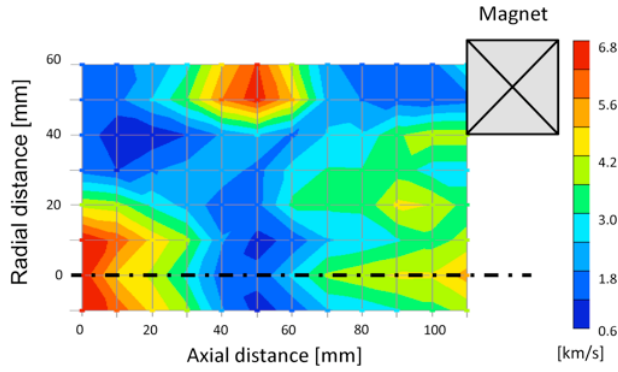
Fig. 11. Contour drawing of the absolute value of the ion velocity in the cusp magnetic field.
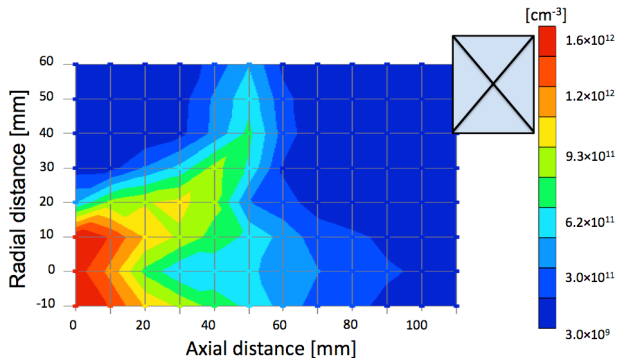

Fig. 12. Contour drawing of the electron density in the cusp magnetic field.
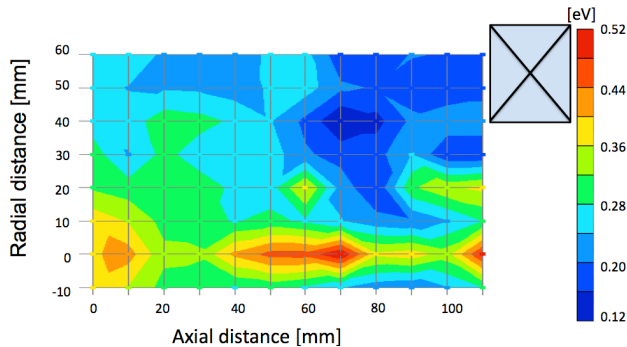

Fig. 13. Contour drawing of the electron temperature in the cusp magnetic field.

Anyway, Fig. 11 indicates that the ion flow is remarkably decelerated near the saddle point of the magnetic field. Meanwhile, the electrons are fully magnetized, and consequently, they tend to flow to the large-r (off-axis) direction rapidly, whereas the ions tend to stay near the axis and to flow to z-direction due to their large inertia. This behavior of charged particles, in turn, results in the attraction of electrons to the on-axis direction near the saddle point. Hence, it is considered that the potential near the saddle point becomes highest in the domain examined.

Next, let us discuss the reason for the plasma potential drop on the axis of $z \geq 70$ mm. The hall parameters show that the electrons are still magnetized in this domain, but that the ions are not. Therefore, in the downstream after the saddle point, the electrons are strongly magnetized again and attracted to the central region, whereas the large inertia of ions causes some "moving-lag" for ions in comparison with the electrons. This makes the potential drop, and again, the ions are accelerated in the subsonic region due to the potential drop and the converging flow channel. This time, the flow is totally subsonic, and consequently, the converging channel accelerates the flow (also see Fig. 8).

Fig. 12 shows the electron density contour. Obviously, we can find sharp density drops at the shock front observed as a dark cone, $z = 10$-30 mm and $r = 0$-20 mm. This density contour also indicates that the flow direction of the charged particles almost agrees with the magnetic lines of force, although the directions do not agree exactly with each other.

Fig. 13 shows the electron temperature contour. What should be noted is that the electron temperature increases from $z = 40$ mm to $z = 60$ mm on axis. We can attribute the increase in the electron temperature mainly to two factors. Firstly, the heating is caused when passing through the shock front, and secondly, the kinetic energy is converted to the thermal energy. That is, the supersonic movement of ions is changed into random motion of each ion due to collisions with residual neutral particles.

We can understand that the variation in the plasma parameters, particularly in the plasma potential and the flowing velocity is mainly caused by the difference between electrons and ions. That is, the electrons are fully magnetized under the present magnetic field, whereas the ions are not magnetized at all.

IV. CONCLUSION

We experimentally studied flowing characteristics of arc-jet plasma through the mirror-type and cusp-type magnetic field. We generated helium arc plasma under atmospheric pressure, followed by supersonic expansion through an anode nozzle into a lower-pressure vessel with a uniform magnetic field, and made the plasma pass through the mirror or the cusp magnetic field. We measured ion Mach number, direction of the ion flow, space potential, electron density and electron temperature by a para-perp type probe and a 4-tip Mach probe.

Based on a discussion of hall parameters of electrons and ions throughout the present experiments, both for the mirror magnetic field and for the cusp magnetic field, the electrons were found to be magnetized, although the ions were not. Therefore, we thought that some diffusion process could occur for ion transport. Basically, the electrons were transported along the magnetic lines of force, whereas the ion transportation was characterized by the Coulomb force, mainly governed by the electron motion.

For the plasma flow along the mirror magnetic field, it was found that the space potential became higher near the radially boundary region and that it became lower near the central axis of the plasma jet.

Concerning the plasma flow along the cusp magnetic field, a cone-shaped dark zone was observed at about 30 mm-downstream region from the first set of magnets. This dark zone was considered to agree with the shock front, where the plasma flow changed to subsonic from supersonic. It was also found that the space potential increased near the saddle point of the magnetic field, followed by a potential drop by about 1 V. This is mainly because the difference in the magnetization between electrons and ions. Electrons tended to come again to the near-axis zone, whereas diffusion across magnetic field became dominant for ions after passing the saddle point in the magnetic field.

References

[1] Y. Ando, S. Tobe, H. Tahara, and T. Yoshikawa, "Creation of temperature non-equilibrium plasma jets by supersonic expansion of DC arc plasma jets and applications of the plasma jets to surface nitriding," *Journal of Japan Thermal Spraying Society,* vol. 36, pp. 38-45, 1999.

[2] T. Shibata, H. Tahara, T. Yasui, Y. Kagaya, and T. Yoshikawa, "Development of electromagnetic acceleration plasma arcjet generators for titanium nitride reactive spray coatings" (in Japanese), *Quarterly Journal of the Japan Welding Society,* vol. 19, pp. 465-471, 2001.

[3] H. Tahara, K. Y. Kagaya, and T. Yoshikawai, "Effects of applied magnetic fields on performance of a quasisteady magnetoplasmadynamic arc," *Journal of Propulsion and Power*, vol. 11, pp. 337-342, 1995.

[4] H. Tahara, Y. Kagaya, and T. Yoshikawa, "Performance and acceleration process of quasisteady magnetoplasmadynamic arcjets with applied magnetic fields," *Journal of Propulsion and Power,* vol. 13, pp. 651-658, 1997.

[5] H. Tahara and Y. Kagaya, "Performance and plasma characteristics of a cusp and divergent-nozzle applied-magnetic-field MPD thruster," in *Proc. 30th International Electric Propulsion Conference*, Florence, Italy, IEPC-2007-335, 2007.

[6] A. Sasoh, D. Ichihara, T. Enoki, and S. Yokota, "Steady-state, applied-field, rectangular magnetoplasmadynamics thruster using hollow cathode," 48th AIAA/ASME/SAE/ASEE Joint Propulsion Conference & Exhibit, AIAA 2012- 4076, 2012.

[7] K. Takahashi and T. Fujiwara, "Ion acceleration enhanced by additional neutralizing electrons in a magnetically expanding double layer plasma," *Physics of Plasmas,* vol. 17, 104505, 2010.

[8] S. Suzuki, M. Akiba, and M. Saito, "2. Comprehending the divertor structure (comprehending the structure of a vacuum vessel and in-vessel components of fusion machines)" (in Japanese), *Journal of Plasma and Fusion Research,* vol. 82, pp. 699-706, 2006.

[9] E. Havlíčková, W. Fundamenski, F. Subba, D. Coster, M. Wischmeier, and G. Fishpool, "Benchmarking of a 1D scrape-off layer code SOLF1D with SOLPS and its use in modelling long-legged divertors," *Plasma Physics and Controlled Fusion,* vol. 55, 065004, 2013.

[10] G. Fishpool, J. Canik, G. Cunningham, J. Harrison, I. Katramados, A. Kirk, M. Kovari, H. Meyer, R. Scannell, and M.-U. Team, "MAST-upgrade divertor facility and assessing performance of long-legged divertors," *Journal of Nuclear Materials,* vol. 438, pp. S356-S359, 2013.

[11] K. Yoshida, T. Kanuma, H. Ichii, A. Nezu, H. Matsuura, and H. Akatsuka, "Flow characteristics of a cold helium arc-jet plasma along open field lines," *IEEJ Transactions on Electrical and Electronic Engineering,* vol. 4, pp. 416-421, 2009.

[12] A. Ando, "Plasma flow measurement : probe method (2. Fundamentals of plasma flow diagnostics, research guidance to fast-flowing plasmas and shock wave)" (in Japanese), *Journal of Plasma and Fusion Research,* vol. 83, pp. 169-175, 2007.

[13] A. Ando, T. Watanabe, T. Watanabe, H. Tobari, K. Hattori, and M. Inutake, "Evaluation of para-perp type mach probe by using a fast flowing plasma," *Journal of Plasma and Fusion Research,* vol. 81, pp. 451-457, 2005.

[14] K. Yoshida, T. Shibata, A. Nezu, H. Matsuura, and H. Akatsuka, "Ion acceleration in arc jet plasma along open field lines," *IEEE Transactions on Plasma Science,* vol. 37, pp. 1414-1418, 2009.

[15] K. Yoshida, T. Shibata, A. Nezu, H. Matsuura, and H. Akatsuka, "Flowing characteristics of cold arc jet plasma along open field lines," *Journal of Plasma and Fusion Research SERIES*, vol. 8, pp. 923-927, 2009.

[16] Y. Nagahara, H. Ichii, K. Yoshida, A. Nezu, H. Matsuura, and H. Akatsuka, "Characteristics of cold argon arc-jet plasma flowing along open-field-line and the effects of collisions on deceleration," *IEEE Transactions on Plasma Science,* vol. 41, pp. 1869-1877, 2013.

[17] H. Akatsuka and M. Suzuki, "Arc-heated magnetically trapped expanding plasma-jet generator," *Review of Scientific Instruments,* vol. 64, pp. 1734-1739, 1993.

[18] K. Kuriki and Y. Arakawa, *Introduction to Electric Propulsion*, Tokyo, Japan: Univ. Tokyo Press, 2003, pp. 69-93 (in Japanese).